Swelling and Shrinking Dynamics of Nematic Elastomers Having Global Director Orientation

Kenji Urayama,* Ryo Mashita, Yuko O. Arai, and Toshikazu Takigawa

Department of Materials Chemistry, Kyoto University, Kyoto 615-8510, Japan

Received July 6, 2006

ABSTRACT: We reveal that the swelling and shrinking of monodomain nematic elastomers in solvents exhibit unusual kinetics owing to the presence of shape and volume variation modes with markedly different rates. A change in the degree of nematic order caused by temperature (*T*) jumps drives a spontaneous macroscopic deformation along the director as well as a change in the chemical potential of the solvent inside the gel. The former yields an almost instantaneous shape variation, whereas the latter induces a slow volume variation governed by the diffusion of polymer networks, such as the swelling of isotropic gels. The markedly different rates of these two modes yield unique kinetics of swelling and shrinking: (1) a pronounced over- or undershoot of the gel dimensions is observed in the direction where the effect of shape variation on the dimensions counters that of the volume variation, and (2) a large dimensional change (more than 50% of the total change) occurs immediately after the *T*-jumps in the direction along which the effects of the two modes on the dimensions harmonize.

Introduction

Nematic elastomers have received considerable attention as soft solid materials possessing nematicity.[1] Their most interesting characteristic is that the molecular alignment of the constituent mesogens directly couples with the macroscopic shape and vice versa. A familiar phenomenon stemming from this characteristic is the macroscopic deformation induced by the nematic−isotropic (N−I) transition of the constituent mesogens between the disordered state and the globally aligned nematic state.[1,2] The nematic elastomers are expected to be promising materials for use in artificial muscles because of their unique stimulus-response behavior.[3] When nematic elastomers are swollen and surrounded by solvents (nematic gels), the N−I transition results in volume as well as shape variations. "Monodomain" nematic gels having global directors undergo a smooth transition between the isotropic swollen state without shape anisotropy and the nematic shrunken state elongated along the director.[4,5] When the swellant possesses nematicity, the orientation of the surrounding solvents also affects the anisotropic swelling.[5] As a consequence, the gel volume exhibits a reentrant temperature (*T*) dependence, whereas the shape anisotropy in the nematic state increases with decreasing *T*. It should be noted that the variation in the nematic order of each nematogen plays a major role in the *T* dependence of the equilibrium volume and shape of the gels.[5−7]

The swelling and shrinking of nematic networks are also expected to exhibit interesting features in their dynamics. In the case of isotropic (nonmesomorphic) gels whose shapes remain similar before and after swelling, no significant anisotropy appears in the swelling dynamics even for long cylindrical and thin disk-shaped gels with large anisotropy in the original shape.[8−10] In contrast, the swelling process of nematic gels whose shapes become dissimilar due to anisotropic swelling inevitably involve a (anisotropic) shape variation mode in addition to the volume variation mode. The swelling dynamics of nematic gels, however, still have not been characterized. The swelling kinetics of "polydomain" nematic gels after the *T*-jumps across the transition temperature was investigated in our previous study.[11] A coupling of the N−I transition and volume change yields interesting kinetics; however, swelling or shrinking proceeds isotropically owing to the absence of a global director in the polydomain textures. Yusuf et al.[12] studied the swelling process of monodomain nematic networks from the dry nematic state to the swollen nematic state at a constant temperature. They observed a finite anisotropy in swelling; however, the volume and shape variation modes were indistinguishable because the degree of nematic order does not change significantly without temperature variations. In the present study, we demonstrate that swelling or shrinking triggered by the *T*-jumps yielding a considerable change in nematic order exhibits an unusual time dependence of the gel dimensions owing to the presence of these two modes.

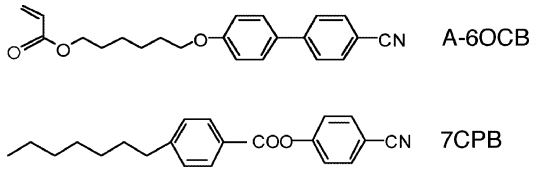

Figure 1. Chemical structures of the reactive mesogenic monomer A-6OCB and nematic solvent 7CPB.

Experimental Section

A side-chain monodomain nematic network was prepared via photopolymerization of an acrylate mesogenic monomer (A-6OCB in Figure 1) with 1,6-hexanediol diacrylate (cross-linker). The cross-linker concentration was 7 mol % in the feed. The photopolymerization was carried out in a glass cell whose surfaces were coated with uniaxially rubbed polyimide layers to achieve a homogeneous alignment of the nematogens. The sample preparation is described in detail in ref 4. The unreacted materials were carefully washed out from the gel by swelling in dichloromethane. After complete deswelling, the rectangular film specimen with a thickness of ca. 20 μm and width and length of ca. 500 μm each was allowed to swell in the low-molecular-mass liquid crystal 4-*n*-heptylbenzoic acid 4-cyanophenyl ester (7CPB in Figure 1) with an N−I transition temperature of 54.2 °C. The quoted purity of 7CPB (Sigma-Aldrich) was at least 99%, and it was used as received without further purification. The N−I transition temperature of the dry nematic network is 110 °C.

The swelling and shrinking processes after the *T*-jumps with various initial and destination temperatures (designated as T_i and

* To whom correspondence should be addressed. E-mail: urayama@rheogate.polym.kyoto-u.ac.jp.

10.1021/ma061507i CCC: $33.50
Published on Web 11/04/2006

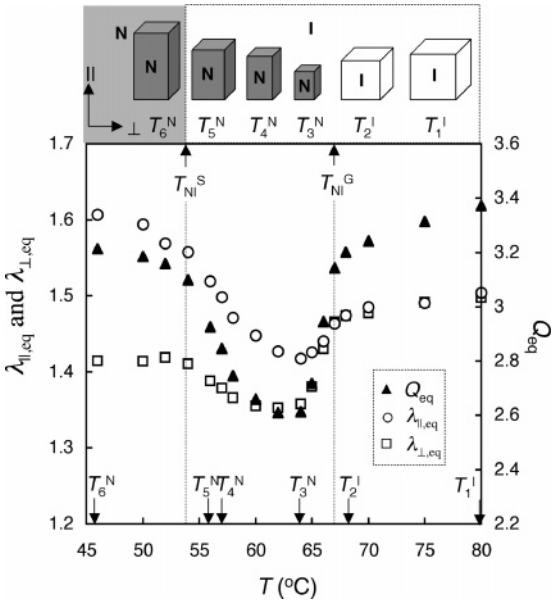

Figure 2. Equilibrium principal ratios (λ_{eq}) in the directions parallel (||) and normal ($\perp$) to the director and the degree of equilibrium swelling (Q_{eq}) as a function of temperature (T) for the nematic network in the nematic solvent. The temperatures T_n ($n = 1, 2, ..., 6$) were selected as the initial and destination temperatures in the T-jump experiments. The transition temperatures of the gel and surrounding solvent are denoted by T_{NI}^G and T_{NI}^S, respectively. The schematic diagram shows the equilibrium volume and shape of the gel at T_n. The dimensional and volume changes in the schematic are enlarged for explanation.

T_d, respectively) were observed using a polarizing optical microscope equipped with a hot stage (Linkam LK-600PM). The surface level of the surrounding solvent in a quartz cell was sufficiently low; therefore, the phase and outline of the gel were distinct when viewed through the microscope (whereas sufficiently high to completely immerse the gel). In the T-jump experiments, the completely swollen gel at T_i was rapidly heated or cooled to T_d at a rate of 130 °C/min. A coolant of a temperature of 0 °C was circulated around the sample cell to achieve rapid cooling. The times required for the changes from T_i to T_d were negligibly small when compared with the time scale of the entire course of interest. The degree of temperature over- or undershoot around T_d after the T-jumps was sufficiently small (less than 0.5 °C).

The dimensions of the gel (d) along the axes parallel (||) and perpendicular ($\perp$) to the director were measured as a function of time after the T-jumps. The first measurement after starting the T-jump ($t = 0$ s) was performed at $t = 30$ s. The principal ratio λ in each direction is defined by

$$\lambda_{||} = d_{||}/d_{||,dry}{}^{I} \tag{1a}$$

$$\lambda_{\perp} = d_{\perp}/d_{\perp,dry}{}^{I} \tag{1b}$$

where $d_{||,dry}{}^{I}$ and $d_{\perp,dry}{}^{I}$ are the dimensions in the corresponding direction of the dry network in the isotropic state at 120 °C. In the dry and isotropic state, the dimensions are almost independent of temperature. The degree of swelling Q for the uniaxially oriented gel is expressed as

$$Q = V/V_{dry} = \lambda_{||}\lambda_{\perp}{}^{2} \tag{2}$$

where V and V_{dry} are the gel volumes in the swollen and dry states, respectively.

Results and Discussion

Equilibrium Phase Diagram. Figure 2 shows the equilibrium values of Q and λ (denoted as Q_{eq} and λ_{eq}) as a function of T for the sample employed in the T-jump experiments. An appreciable difference in the equilibrium swelling and phase behaviors in the cooling and heating processes was not observed. The result observed in this figure is similar to that in our previous study.[5] The N−I transition of the gel occurs at T_{NI}^G (67 °C); below this temperature, the nematic network and the solvent inside the gel form a single nematic phase. At T_{NI}^S, the solvent outside the gel undergoes an N−I transition. The T dependence of the equilibrium volume and shape is schematically shown in the figure. In the totally isotropic regime of $T > T_{NI}^G$, the gel is equally swollen in each direction ($\lambda_{||,eq} = \lambda_{\perp,eq}$). The nematic ordering at T_{NI}^G drives an elongation along the director ($\lambda_{||,eq} > \lambda_{\perp,eq}$) as well as a reduction in the volume. In the regime of $T_{NI}^G > T > T_{NI}^S$, where the phases inside and outside the gel are nematic and isotropic, respectively, the volume increases again and the shape anisotropy increases upon cooling. In the totally nematic regime of $T < T_{NI}^S$, swelling is anisotropic, whereas the volume is as large as that in the totally isotropic regime.

The six temperatures T_n ($n = 1, 2, ..., 6$) in the figure were selected as the initial (T_i) and destination temperatures (T_d) in the T-jump experiments. The superscripts I and N denote the equilibrium phases of the gel (I: isotropic; N: nematic) at the corresponding temperature.

Swelling and Shrinking Accompanying the Nematic−Isotropic Transition Driven by the T-Jumps of $T_1^I \leftrightarrow T_4^N$. The fully swollen isotropic gel at T_1^I (80 °C) and nematic gel at T_4^N (57 °C) have almost the same length along the director [$\lambda_{||,eq}(T_1^I) \approx \lambda_{||,eq}(T_4^N)$], whereas they differ in $\lambda_{\perp,eq}$ (and Q_{eq}), as shown in Figure 2. On the basis of this difference in the equilibrium shapes at T_1^I and T_4^N, it is expected that $\lambda_{\perp}$ changes but $\lambda_{||}$ remains almost constant following the T-jumps between the two temperatures. We show that the actual behavior is more complicated and interesting than the expected behavior.

Figure 3a shows the time (t) dependence of λ and Q during the shrinking process driven by the T-jump of $T_1^I \rightarrow T_4^N$. In the figure, the data at $t = 0$ correspond to the equilibrium values for the isotropic gel at T_1^I (i.e., before the T-jump). The T-jump to T_4^N results in a rapid and uniform formation of a monodomain nematic phase over the entire sample, which completes at $t \approx 10$ s; this was confirmed by polarized optical microscopy. The time required for this T-jump was as large as 10 s. Interestingly, the gel elongates along the appeared director along with the formation of the monodomain nematic phase. The resulting $\lambda_{||}$ exceeds the initial and final values [$\lambda_{||,eq}(T_1^I) \approx \lambda_{||,eq}(T_4^N) \approx 1.5$]. This yields an overshoot of $\lambda_{||}(t)$ during the shrinking process: $\lambda_{||}(t)$ exhibits a maximum in the short-time region and slowly decreases to the equilibrium value at T_4^N. Meanwhile, $\lambda_{\perp}$ decreases toward the equilibrium value without an apparent anomaly; however, it should be noted that $\lambda_{\perp}$ exhibits a considerable reduction (almost 50% of the total reduction) when nematic ordering occurs. This can mainly be attributed to the lateral shrink due to the instantaneous elongation along the appeared director. This shrinking process with the overshoot of $\lambda_{||}$ is schematically shown in Figure 3d.

Figure 3b shows $\lambda(t)$ and $Q(t)$ during swelling after the T-jump of $T_4^N \rightarrow T_1^I$. Similar to the T-jump of $T_1^I \rightarrow T_4^N$, $\lambda_{||}(t)$ is not constant during swelling. The N → I transition in the gel occurs uniformly over the entire sample without an appreciable delay after the completion of the T-jump ($t \approx 10$ s). The disappearance of the global director simultaneously results in compression of the gel in the direction along the original director. This leads to an undershoot of $\lambda_{||}(t)$ in the swelling process. The principal ratio $\lambda_{\perp}$ increases toward the equilibrium value at T_1^I; however, it grows considerably (ca. 70% of the

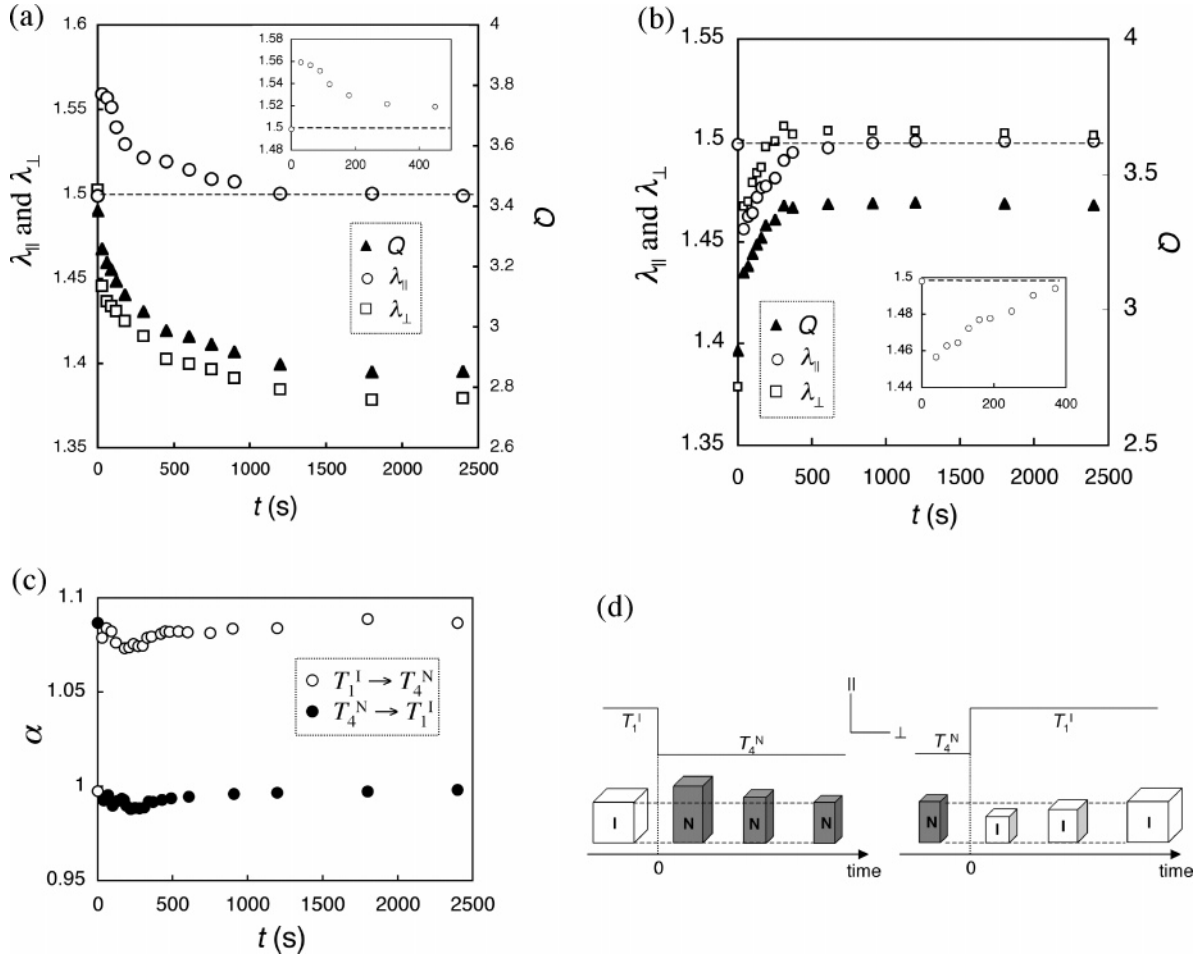

Figure 3. Principal ratios (λ) in the directions parallel (||) and normal ($\perp$) to the director and the degree of swelling (Q) as a function of time (t) after the T-jumps of (a) T_1^I (80 °C) → T_4^N (57 °C) and (b) $T_4^N \rightarrow T_1^I$. The equilibrium gels at T_1^I and T_4^N have almost the same value of $\lambda_{\parallel}$. The insets show $\lambda_{\parallel}(t)$ in the short-time region. The N−I transitions over the entire sample complete at $t \approx 10$ s after both the T-jumps. (c) Shape anisotropy ($\alpha = \lambda_{\parallel}/\lambda_{\perp}$) as a function of t. (d) Schematic diagrams of the shrinking process with the overshoot of $\lambda_{\parallel}$ (left) and the swelling process with the undershoot of $\lambda_{\parallel}$ (right). The dimensional and volume variations in the figure are enlarged for explanation.

total increase) when the N → I transition occurs. This considerable increase in $\lambda_{\perp}$ primarily results from the lateral expansion due to the spontaneous compression along the original director.

The degree of the shape anisotropy of the gel is evaluated by the ratio of $\lambda_{\parallel}$ and $\lambda_{\perp}$ as follows:

$$\alpha = \lambda_{\parallel}/\lambda_{\perp} \tag{3}$$

Figure 3c shows $\alpha(t)$ for these T-jumps. For both the cases, α reaches the equilibrium value at T_d immediately after the T-jump. This implies that almost the entire shape variation occurs due to the instantaneous deformation; during the later stages, volume variation is dominant without any appreciable further shape variation.

Swelling and Shrinking Driven by the T-jumps of $T_3^N \leftrightarrow T_6^N$ within the Nematic Regime. The T-jumps within the nematic regime of $T < T_{NI}^G$ also drive a finite change in the degree of nematic order that yield volume and shape variations in the gel. The ascending or descending temperature in the T-jump induces a decrease or increase in the nematic order of the gel, respectively, in a qualitative manner similar to that in low-molecular-mass liquid crystals.[1]

The equilibrium principal ratios $\lambda_{\parallel,eq}$ and $\lambda_{\perp,eq}$ at T_6^N (46 °C) are greater than those at T_3^N (64 °C). Figure 4a shows $\lambda(t)$ and $Q(t)$ during swelling after the T-jump of $T_3^N \rightarrow T_6^N$. Immediately after the T-jump, $\lambda_{\perp}$ decreases below $\lambda_{\perp,eq}(T_3^N)$, whereas a noticeable increase is observed in $\lambda_{\parallel}$ (almost 50% of the total increase). These considerable variations in $\lambda_{\parallel}$ and $\lambda_{\perp}$ result from the instantaneous stretching along the director caused by an increase in the nematic order of the gel. This T-jump also induces swelling that increases the dimensions in all the directions. In the direction normal to the director, swelling changes the dimension opposite to the spontaneous deformation. In addition, the time scale of swelling is considerably greater than that of the spontaneous deformation, as shown in a later section. As a consequence, $\lambda_{\perp}(t)$ exhibits a pronounced undershoot behavior (Figure 4d).

Figure 4b shows $\lambda(t)$ and $Q(t)$ during shrinking after the T-jump of $T_6^N \rightarrow T_3^N$. In this case, $\lambda_{\perp}(t)$ exhibits an overshoot behavior. This T-jump induces a decrease in the nematic order of the gel that drives a spontaneous compression along the director and a decrease in the volume. As a result of the lateral expansion due to the macroscopic compression along the director, $\lambda_{\perp}$ in the short-time region increases above $\lambda_{\perp}$, eq(T_6^N). This spontaneous compression also results in a considerable decrease in $\lambda_{\parallel}$ (ca. 60% of the total decrease) without an appreciable delay after the T-jump. The results are explained qualitatively in a manner similar to those in Figure 4a by replacing the terms "stretching" and "swelling" with "compression" and "shrinking", respectively.

Figure 4c shows the values of $\alpha(t)$ for these T-jumps. As in the case of the T-jumps across T_{NI}^G (Figure 3c), almost the entire changes in α occur instantaneously after the temperature

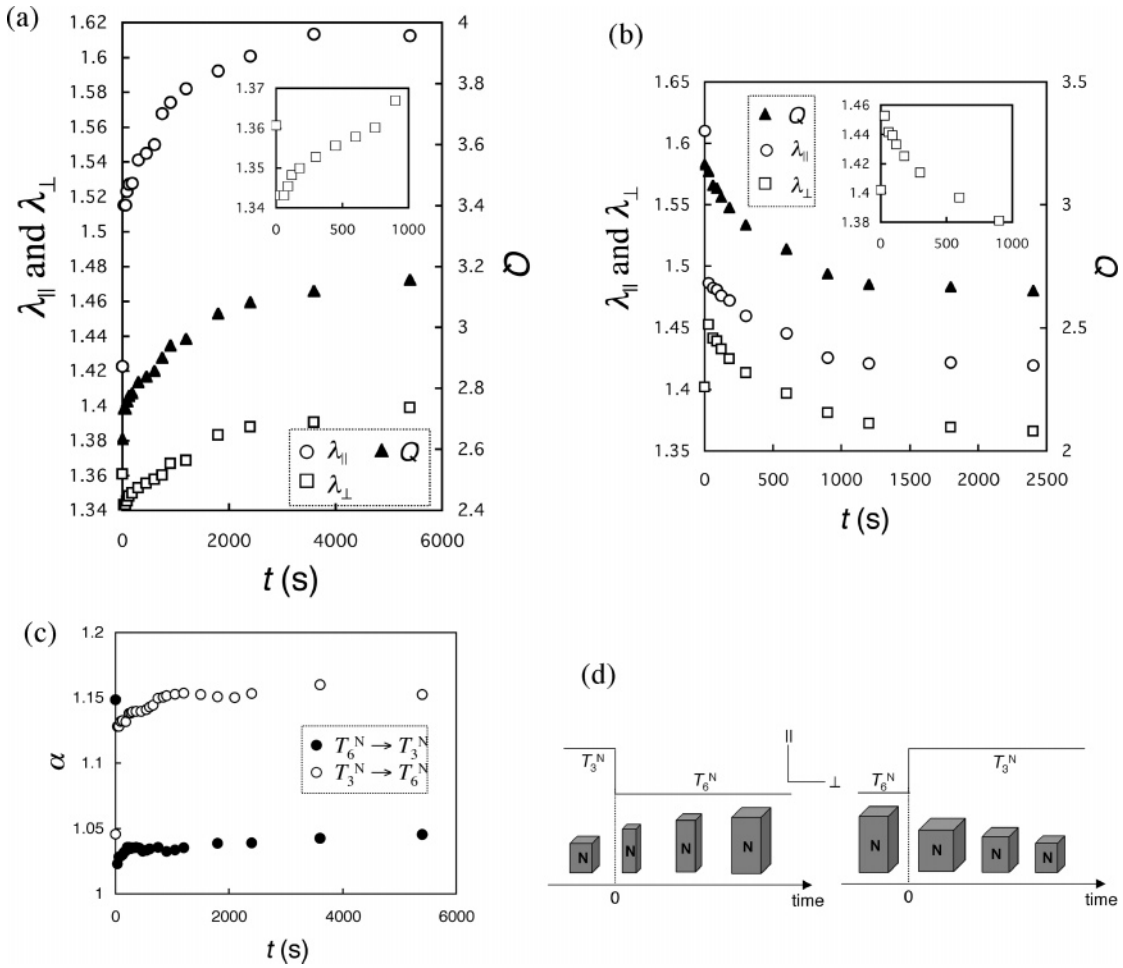

Figure 4. Principal ratios (λ) in the directions parallel (||) and normal ($\perp$) to the director and the degree of swelling (Q) as a function of time (t) after the T-jumps of (a) T_3^N (64 °C) → T_6^N (46 °C) and (b) T_6^N → T_3^N. The insets show $\lambda_{\perp}(t)$ in the short-time region. (c) Shape anisotropy ($\alpha = \lambda_{\parallel}/\lambda_{\perp}$) as a function of t. (d) Schematic diagrams of the swelling process with the undershoot of $\lambda_{\perp}$ (left) and shrinking process with the overshoot of $\lambda_{\perp}$ (right). The dimensional and volume variations in the figure are enlarged for explanation.

variations. For the T-jump of $T_3^N \rightarrow T_6^N$, a slight increase in α during a later stage is recognizable. This may imply the presence of a formation process of a further ordered structure coupled to swelling.

Shape Change with Almost No Volume Change Driven by the T-Jumps of $T_2^I \leftrightarrow T_6^N$. The equilibrium swollen gels at T_2^I (68 °C) and T_6^N (46 °C) are similar in volume (Q_{eq}), but they differ in shape ($\lambda_{||,eq}$ and $\lambda_{\perp,eq}$). The T-jumps between T_2^I and T_6^N are expected to induce shape changes without volume change and reveal only the shape variation mode. Parts a and b of Figure 5 show $\lambda(t)$ and $Q(t)$ after the T-jumps of $T_6^N \rightarrow T_2^I$ and $T_2^I \rightarrow T_6^N$, respectively. The N → I and I → N transitions rapidly complete at $t \approx 10$ s. From this figure, it can be observed that the shape variations occur with almost no change in volume (Q), as expected. It should be noted that the total processes complete rapidly, and they are at least 2 orders of magnitude faster than the processes involving a finite volume change in Figures 3 and 4. It is difficult to accurately evaluate the characteristic time for the shape variation mode on the basis of the data in Figure 5. Because of an unavoidable finite difference in Q_{eq} for T_i and T_d, it is not possible to completely exclude the volume change process in the experiments. The presence of a finite volume change delays the entire process. The results in Figure 5, however, are sufficient to confirm that the shape variation mode is considerably faster than the volume variation mode. The shape variation mode observed in "swollen" nematic elastomers is substantially similar to the familiar spontaneous deformation[1−3] of "dry" nematic elastomers without volume variation that occurs almost instantaneously after the temperature changes.

Mechanism of Over- and Undershoots in Gel Dimensions during Swelling and Shrinking. These results demonstrate that the swelling and shrinking dynamics of monodomain nematic gels comprises two modes, namely, volume and shape variation modes. The over- and undershoots in the sample dimensions appear as a result of a marked difference in the characteristic times with regard to the two modes. A change in the nematic order of the gel (caused by the T-jumps) yields (1) a spontaneous deformation (shape variation) and (2) a change in the chemical potential of the solvent inside the gel that induces swelling or shrinking (volume variation). The former effect (1) occurs almost instantaneously after the temperature change. An increase (or decrease) in the nematic order induced by a temperature drop (or rise) drives a stretching (or compression) along the director. This deformation substantially involves no appreciable volume change because the gels are mechanically incompressible similar to cross-linked rubbers.

The latter effect (2) thermodynamically drives a finite volume change (except special cases such as the T-jumps of $T_2^I \leftrightarrow T_6^N$) in order to balance the chemical potentials of the solvents inside and outside the gel. The kinetics of the volume change is governed by the diffusion of polymer networks. Many studies[8,9,13−17] on the swelling kinetics of nonmesomorphic gels have revealed that the diffusion of networks is a slow process characterized by the diffusion constant (D) of the order of 10^{-11}

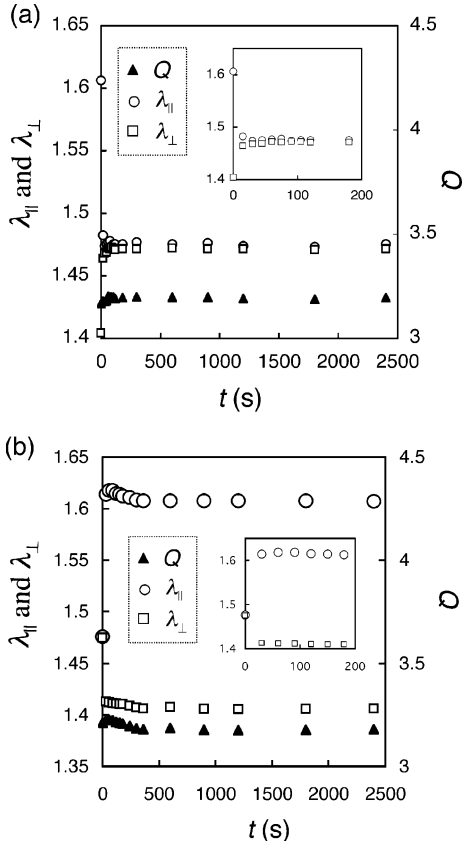

Figure 5. Principal ratios (λ) in the directions parallel (||) and normal ($\perp$) to the director and the degree of swelling (Q) as a function of time (t) after the T-jumps of (a) T_6^N (46 °C) → T_2^I (68 °C) and (b) T_2^I → T_6^N. The equilibrium gels at T_2^I and T_6^N have almost the same value of Q. The insets show $\lambda_{||}(t)$ and $\lambda_{\perp}(t)$ in the short-time region. The N−I transitions over the entire sample complete at $t \approx 10$ s after both the T-jumps.

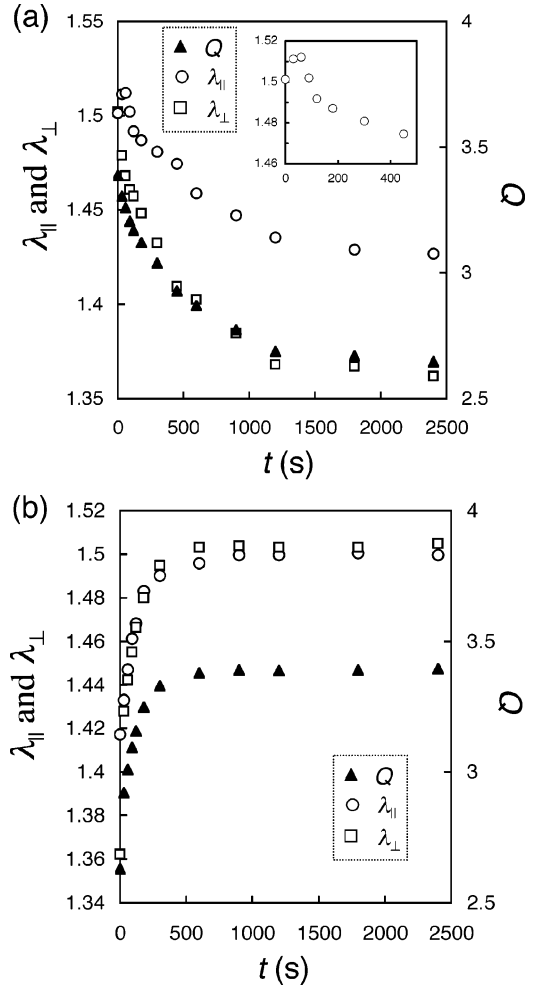

Figure 6. Principal ratios (λ) in the directions parallel (||) and normal ($\perp$) to the director and the degree of swelling (Q) as a function of time (t) after the T-jump of (a) T_1^I (80 °C) → T_3^N (64 °C) and (b) T_3^N → T_1^I. The inset shows $\lambda_{||}(t)$ in the short-time region.

or 10^{-12} m^2/s. In a later section, it will be shown that D of the present system also has the same order of magnitude. The volume variation is composed of many modes with a broad distribution of relaxation times,[13] and the fast modes yield a finite change in Q in the short-time region. A finite contribution of the fast volume variation modes may weaken or mask the over- or undershoot of the sample dimensions when the total volume change (ΔQ) is sufficiently large. For instance, in the T-jumps of $T_1^I \leftrightarrow T_3^N$ across T_{NI}^G causing the greatest ΔQ in the present system, the overshoot of $\lambda_{||}$ is less pronounced (Figure 6a) and the undershoot of $\lambda_{||}$ is not visible (Figure 6b); this is in contrast to the cases of the similar T-jumps of $T_1^I \leftrightarrow T_4^N$ across T_{NI}^G that yield a smaller ΔQ (Figure 3). In these cases, it should be noted that the shape and volume variations act to change $\lambda_{||}$ in the opposite manner; the large volume changes can yield a counter effect comparable to or exceeding the dimensional change due to the spontaneous deformation.

Diffusion Constants of Swelling and Shrinking. In this section, we discuss the diffusion constant that characterizes the volume variation mode. The volume variation mode governs the swelling or shrinking process in the long-time region after the spontaneous deformation. The swelling kinetics generally obey a multiexponential-type relaxation:[13]

$$\frac{\Delta\lambda(t)}{\Delta\lambda} = \sum_{i=1} A_i \exp\left(-\frac{t}{\tau_i}\right) \tag{4}$$

where $\Delta\lambda(t) = \lambda(t) - \lambda(\infty)$, $\Delta\lambda = \lambda(0) - \lambda(\infty)$, and A_i and τ_i are the strength and characteristic time of the ith mode,

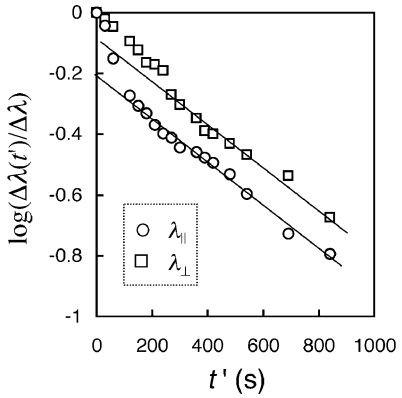

Figure 7. Semilog plot of $\Delta\lambda(t')/\Delta\lambda$ vs t' for shrinking after the T-jump of T_1^I (80 °C) → T_4^N (57 °C), where $\Delta\lambda(t') = \lambda(t') - \lambda(\infty)$, $\Delta\lambda = \lambda(t' = 0) - \lambda(\infty)$, and t' ($= t - t_{peak}$) is the time elapsed after the spontaneous deformation. The inverse of the slope yields the longest characteristic times $\tau = 6.2 \times 10^2$ s and 5.8×10^2 s for $\lambda_{||}$ and $\lambda_{\perp}$, respectively.

respectively. When $\lambda(t)$ exhibits an over- or undershoot, we replace t in eq 4 with the elapsed time ($t' = t - t_0$) after the spontaneous deformation completes (t_0). For simplicity, we employ the time at the peak of $\lambda(t)$ (t_{peak}) as t_0. Figure 7 shows the semilog plot of $(\Delta\lambda(t')/\Delta\lambda)$ vs t' for the shrinking process with the overshoot of $\lambda_{||}$ after the T-jump of $T_1^I \rightarrow T_4^N$. In the sufficiently long-time region, a good linear correlation is observed for both $\lambda_{||}$ and $\lambda_{\perp}$. The longest characteristic time (τ

Table 1. Diffusion Constants in the Directions Parallel (∥) and Normal (⊥) to the Director

T-jump	$D_{\parallel} \times 10^{12}$ (m^2 s^{-1})	$D_{\perp} \times 10^{12}$ (m^2 s^{-1})
$T_1^I \rightarrow T_4^N$	1.2	1.3
$T_4^N \rightarrow T_1^I$	5.1	8.8
$T_1^I \rightarrow T_3^N$	1.0	1.3
$T_3^N \rightarrow T_1^I$	4.5	6.2
$T_3^N \rightarrow T_5^N$	1.3	0.90
$T_5^N \rightarrow T_3^N$	1.2	1.1
$T_3^N \rightarrow T_6^N$	0.68	0.54
$T_6^N \rightarrow T_3^N$	1.6	1.2

$\equiv \tau_1$) is evaluated from the inverse of the slope. As the thickness of the film sample is 1 order of magnitude smaller than the other two dimensions ($d_{\parallel}$ and $d_{\perp}$), the film thickness is the dimension that governs the diffusion of the polymer networks.[8,9] On the basis of the kinetic theory of swelling of isotropic gels,[8−10,13] the apparent diffusion constant is estimated as

$$D \approx d_t^2/\tau \tag{5}$$

where d_t is the equilibrium thickness at T_d and the numerical coefficient is not considered for simplicity. The applicability of eq 5 to anisotropic networks is not evident; however, its use for the present qualitative discussion is tolerable because no theory for swelling kinetics of anisotropic networks has not yet been established. The values of *D* for each *T*-jump evaluated in a similar manner are listed in Table 1.

In Figure 7, a finite deviation from the linear correlation in the short-time region is observed for $\lambda_{\parallel}(t')$. This deviation may be attributed to the contributions of the fast modes of $i \geq 2$ in eq 4; however, the evaluation of the fast modes from Figure 7 is not straightforward because the degree of deviation strongly depends on the selection of t_0 and the fast modes of volume variation coexist with the shape variation mode in the short-time region. It should be emphasized that the characteristic at long times such as τ is insensitive to the selection of t_0, unlike that at the short times.

Figure 8 shows the values of $D_{\parallel}$ and $D_{\perp}$ for each *T*-jump. As a whole, the values of *D* (on the order of 10^{-12} m^2 s^{-1}) are in a similar order to those for isotropic gels.[8,9,13−17] It appears that there exists no significant difference in $D_{\parallel}$ (filled symbols) and $D_{\perp}$ (open symbols) at each *T*-jump for the present system. The data for the networks with higher nematic anisotropy in network chains (yielding larger shape anisotropy) will be further needed to elucidate if a finite anisotropy is truly absent in the slow volume variation mode. This is a matter of our future investigation. The values of *D* for swelling after the two *T*-jumps of $T_4^N \rightarrow T_1^I$ and $T_3^N \rightarrow T_1^I$ are ca. 5 times greater than those for the other processes. The destination temperatures T_d (T_1^I) of these two *T*-jumps belong to the isotropic state of the gel, whereas T_d of all the other *T*-jumps are in the nematic state. Swelling and shrinking in the nematic state involve the process of nematic ordering or the formation of a further ordered structure. The formation process of the ordered structure is expected to delay swelling or shrinking when compared with those in the isotropic state that accompany no structure formation. The values of *D* for swelling after the *T*-jump of $T_3^N \rightarrow T_6^N$ are slightly less than those for the other *T*-jumps. The surrounding solvent at the destination temperature T_6^N ($< T_{NI}^S$) of this *T*-jump is in the nematic state, whereas those at T_d ($> T_{NI}^S$) of all the other *T*-jumps are in the isotropic state. A slightly greater viscosity of the surrounding swellant in the nematic state yields a slower swelling than that in the isotropic state; this is because *D* is inversely proportional to the friction coefficient between the network and swellant.[8−10,13−18]

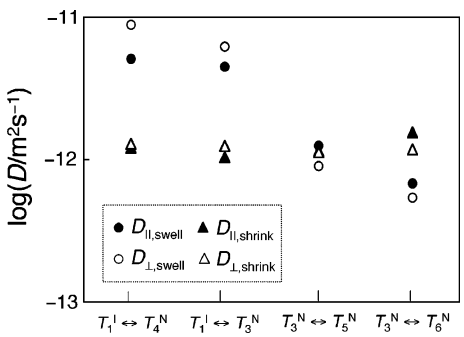

Figure 8. Diffusion constants (*D*) in the direction parallel (∥) and normal (⊥) to the director for each *T*-jump.

Conclusions

The swelling and shrinking dynamics of the nematic elastomers having a global director comprises the shape and volume variation modes with markedly different characteristic times. A change in the degree of nematic order due to the *T*-jumps drives a spontaneous deformation along the director and a change in the chemical potential of the solvent inside the gel. The former causes a rapid elongation or compression along the director that occurs simultaneously with the temperature variation when the nematic order increases or decreases, respectively. The latter induces a volume variation (swelling or shrinking) that is a slow process governed by the diffusion of polymer networks, such as swelling of isotropic gels. The remarkable difference in the characteristic times with regard to these two modes yields an over- or undershoot of the gel dimensions in the direction where the spontaneous deformation and volume variation act to change the dimension in the opposite manner. In the direction where these two effects on the dimension synchronize, a large dimensional change (more than 50% of the total change) occurs with almost no delay after the *T*-jump.

Acknowledgment. The authors are grateful to Ciba Specialty Chemicals Co. for the provision of a photoinitiator. This work was partly supported by a grant from the Murata Science Foundation, a Grant-in-Aid (No. 18350117), and the 21st Century COE program "COE for a United Approach to New Materials Science" from the Ministry of Education, Culture, Sports, Science and Technology, Japan.

References and Notes

(1) Warner, M.; Terentjev, E. M. *Liquid Crystal Elastomers*; Oxford University Press: Oxford, 2003.
(2) Küpfer, J.; Finkelmann, H. *Macromol. Chem., Rapid Commun.* **1991**, *12*, 717.
(3) Thomsen, D. L.; Keller, P.; Nacri, J.; Pink, R.; Jeon, H.; Shenoy, D.; Ratna, B. R. *Macromolecules* **2001**, *34*, 5868.
(4) Urayama, K.; Arai, Y. O.; Takigawa, T. *Macromolecules* **2005**, *38*, 3469.
(5) Urayama, K.; Arai, Y. O.; Takigawa, T. *Macromolecules* **2005**, *38*, 5721.
(6) Wang, X. J.; Warner, M. *Macromol. Theory Simul.* **1997**, *6*, 37.
(7) Matsuyama, A.; Kato, T. *J. Chem. Phys.* **2002**, *116*, 8175.
(8) Peters, A.; Candau, S. J. *Macromolecules* **1988**, *21*, 2278.
(9) Li, Y.; Tanaka, T. *J. Chem. Phys.* **1990**, *92*, 1365.
(10) Yamaue, T.; Doi, M. *J. Chem. Phys.* **2005**, *122*, 084703.
(11) Urayama, K.; Arai, Y. O.; Takigawa, T. *Macromolecules* **2004**, *37*, 6161.
(12) Yusuf, Y.; Ono, Y.; Sumisaki, Y.; Cladis, P. E.; Brand, H. R.; Finkelmann, H.; Kai, S. *Phys. Rev. E* **2004**, *69*, 021710.
(13) Tanaka, T.; Fillmore, D. *J. Chem. Phys.* **1979**, *70*, 1214.
(14) Matsuo, S. E.; Tanaka, T. *J. Chem. Phys.* **1988**, *89*, 1695.
(15) Hakiki, A.; Herz, J. E. *J. Chem. Phys.* **1994**, *101*, 9054.
(16) Hirose, H.; Shibayama, M. *Macromolecules* **1998**, *31*, 5336.
(17) Takahashi, K.; Takigawa, T.; Masuda, T. *J. Chem. Phys.* **2004**, *120*, 2972.
(18) Tanaka, T.; Hocker, L.; Benedek, G. *J. Chem. Phys.* **1973**, *59*, 5151.

MA061507I